Kapal: Jurnal Ilmu Pengetahuan dan Teknologi Kelautan
(Kapal: Journal of Marine Science and Technology)
journal homepage : http://ejournal.undip.ac.id/index.php/kapal
2301-9069 (e)
1829-8370 (p)

The TLP 2-DOF as an alternative model for extreme wave application

Jamiatul Akmal[1)*], Asnawi Lubis[1)], Novri Tanti[1)], Nuryanto[1)], Adam Wisnu Murti[1)],

[1)]Department of Mechanical Engineering, Universitas Lampung, Lampung, Indonesia
[*)]Corresponding Author : jamiatul.akmal@eng.unila.ac.id

Article Info

Keywords:
TLP;
2-DOF system;
Dynamic Vibration Absorber;
Optimization;
RAO;

Article history:
Received: 09/03/2021
Last revised: 04/05/2021
Accepted: 06/05/2021
Available online: 06/05/2021
Published: 30/06/2021

DOI:
https://doi.org/10.14710/kapal.v18i2.37187

Abstract

Tension Leg Platform (TLP) is an offshore platform structure used for deep-sea oil and gas exploration. The main structure of the TLP consists of a deck, pontoon, mooring system, and foundation. TLP operates in a balance of buoyancy, structural weight, and mooring tension. The problem is the construction of TLP in the deep sea, where sometimes extreme waves appear could damage the TLP structure. This paper proposes a new model of TLP that is more stable to extreme waves. The method is to separate the mass of the deck and the mass of the pontoon into two flexible parts, which are connected by a cantilever spring system. Thus the TLP motion becomes two degrees of freedom (TLP 2-DOF). Using the dynamic vibration absorber (DVA) method, the ratio of the deck mass, pontoon mass, and spring stiffness are adjusted so that the primary mass movement is minimal. Furthermore, the ratio of the amplitude of the deck movement as the primary mass to the wave amplitude is analyzed, which is known as the operator response amplitude (RAO). The results showed that the TLP 2-DOF model was more stable. As an illustration, at resonance conditions, this model can reduce RAO 67%.

Copyright © 2021 KAPAL : Jurnal Ilmu Pengetahuan dan Teknologi Kelautan. This is an open access article under the CC BY-SA license (https://creativecommons.org/licenses/by-sa/4.0/).

1. Introduction

Tension Leg Platform (TLP) is an offshore platform that is a "compliant structure," floating above sea level because the buoyancy force is greater than the structure's weight. The main components of the TLP are the pontoon, deck, mooring system, and foundation. The deck position is above sea level in the installed condition while the pontoon is submerged in seawater. The overall structure is tethered to the seabed by mooring ropes. TLP is usually used for deep-sea oil/gas exploration activities. In the past, the TLP was installed at a depth of only 147 m [1], and now TLP has been installed at a depth of more than 1500 m [2].

In the operation of TLP in the deep sea, sometimes there are extreme waves that look strange and are "out of nowhere" [3]. For example, in the South China Sea, there are frequent extreme waves known as internal waves. Internal waves are floating waves caused by variations in water density, propagating in the boundary layer of warm water and cold water below. It can propagate in many ways, including short regular waves, cnoidal and solitary waves, and internal tidal waves [4]. Recently, extreme waves have become a concern because it has the potential to damage structures [5], [6]. For example, in 2004-2005, hurricanes Ivan, Katrina, and Rita in the Gulf of Mexico destroyed 126 offshore structures and damaged 83 others [7].

Researchers have also attempted to study the relationship between extreme waves and dynamic TLP responses. For example, simulation and analysis on rogue wave's impact and their effect on angle and rope tension have been carried out. The interaction between extreme waves and TLP results in complex dynamics, affecting buoyancy, rope tension, and rotational motion [3]. In addition, the dynamic behavior of TLP under extreme waves has been analyzed. It is known that the dynamic response of the TLP is sensitive to extreme waves at high degrees of freedom and an operating frequency nearly the same as the natural wave frequency [8]. This phenomenon is known as resonance. The TLP design should avoid the resonance phenomenon by designing a natural frequency not close to the ocean wave frequency.

Many designers have carried out many efforts to improve the design concept. Among them, modifying the TLP geometry to be triangular [9], adding and adjusting the mass of dampers [10], and proposing a new model of mooring system configuration [11]. In addition, some propose a design for tension-leg twin platform structural systems [10]. However, besides having advantages, those design concepts also have several weaknesses. For example, the Tension-leg twin platform structural systems design depends on the distance of the two pontoon and wavelength, which increases the resulting

dynamic response [13]. For these reasons, this study will discuss a new design that is different from the previous designs, called the Tension Leg Platform of Two Degree of Freedom (TLP 2-DOF), which is relatively more stable to wave force.

Suppose the deck and pontoon form a single unit into a rigid body in the existing model, then in the proposed TLP 2-DOF model. In that case, the deck and pontoon are made into two separate masses connected by a cantilever spring system. Thus its construction can be regarded as a system of two degrees of freedom. The composition of the deck mass, pontoon mass, and spring stiffness can be adjusted for minimal primary mass response[14]. This method is known as dynamic vibration absorber / DVA [15], [16]. The dynamic response is expressed in non-dimensional quantities, namely the ratio of the amplitude of deck motion to wave amplitude, known as the response amplitude operator / RAO [17].

2. Methods

2.1. Models and assumptions

Figure 1 (a) and Figure 1 (b) show the TLP existing model and the TLP 2-DOF model, respectively. Each model was made in comparable sizes and under the same test conditions. Furthermore, the test was carried out on a pool equipped with a set of wave generator mechanisms, as shown in Figure 2. The dimensions of each model and the dimensions of the test pool can be seen in Table 1. To see the new model's performance, the dynamic response was compared by measuring the horizontal motion (x-direction) on each deck. Measurements were made using an ultrasonic sensor equipped with a data acquisition system.

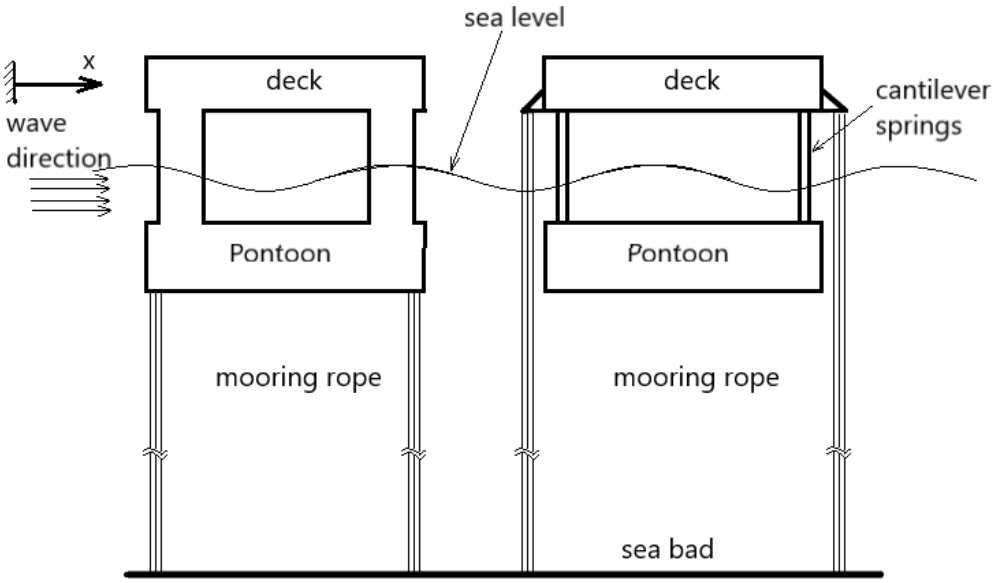

(a) (b)

Figure 1. TLP (a) The Existing Model and (b) The 2-DOF Model

Table 1. Dimensions of each model

Description	Syimbol	Unit	TLP 2-DOF Model	Existing Model
Pontoon				
Length		mm	200	200
Wide		mm	200	200
Height		mm	60	60
Mass	m_p	kg	0,9	0,9
Deck				
Length (mm)		mm	200	200
Wide		mm	200	200
Height		mm	50	50
Mass	m_d	kg	0,3	0,3
Pool				
Length		mm	2000	
Wide		mm	600	
Height		mm	800	
Water level/height	h	mm	600	
Wave direction			x-direction	
Excitation frequency	ω		9,77 rad/s	

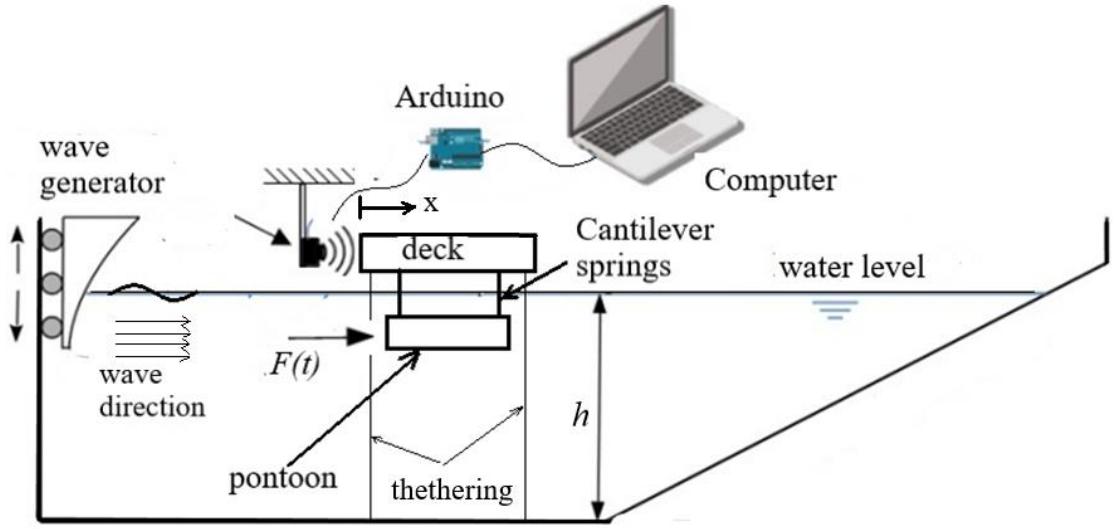

Figure 2. Experiment test set-up

2.2. Mathematical model for determining natural frequencies

Determining the natural frequency is necessary to anticipate the resonance phenomenon during operation. The new model consists of three main components; deck, spring and pontoon, which have mass m_d, m_k and m_p, respectively. The analysis is carried out referring to the free body diagram (FDB) shown in Figure 3.

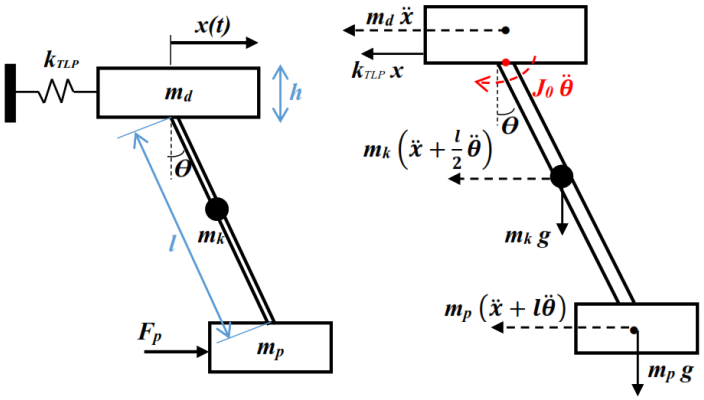

Figure 3. Free Body Diagram of TLP 2-DOF model

If the damping factor of the structure is neglected, the Eq.s of linear and angular motion are as written in Eq. (1) and Eq. (2), respectively. Here x and $\ddot{x}$ is linear displacement and linear acceleration in the x-axis direction, respectively, while θ and $\ddot{\theta}$ Are rotational displacement and rotational acceleration, respectively. In addition, k_{TLP} It is a stiffness factor of the system.

$$\begin{aligned} m_d\ddot{x} + m_k\left(\ddot{x} + \frac{l}{2}\ddot{\theta}\right) + m_p(\ddot{x} + l\ddot{\theta}) + k_{TLP}x = 0 \\ (m_d + m_k + m_p)\ddot{x} + \left(m_k\frac{l}{2} + m_p l\right)\ddot{\theta} + k_{TLP}x = 0 \end{aligned} \tag{1}$$

$$\begin{aligned} J_0\ddot{\theta} - m_d\frac{h}{2}\ddot{x} + m_k\left(\ddot{x} + \frac{l}{2}\ddot{\theta}\right)\frac{l}{2} + m_p(\ddot{x} + l\ddot{\theta})l + m_k g\frac{l}{2}sin\theta \\ + m_p g l\, sin\theta = 0 \\ m_k\frac{l^2}{12}\ddot{\theta} + \left(-m_d\frac{h}{2} + m_k\frac{l}{2} + m_p l\right)\ddot{x} + \left(m_k\frac{l^2}{4} + m_p l^2\right)\ddot{\theta} \\ + m_k g\frac{l}{2}sin\theta + m_p g l\, sin\theta = 0 \end{aligned} \tag{2}$$

$$\begin{aligned} \left(-m_d\frac{h}{2} + m_k\frac{l}{2} + m_p l\right)\ddot{x} + \left(m_k\frac{l^2}{3} + m_p l^2\right)\ddot{\theta} \\ + \left(m_k g\frac{l}{2} + m_p g l\right)\theta = 0 \end{aligned}$$

With the stiffness matrix method, Eq. (1) and Eq. (2) can be solved to obtain Eq. (3).

$$\begin{bmatrix} m_d + m_k + m_p & m_k\frac{l}{2} + m_p l \\ -m_d\frac{h}{2} + m_k\frac{l}{2} + m_p l & m_k\frac{l^2}{3} + m_p l^2 \end{bmatrix}\begin{Bmatrix}\ddot{x}\\ \ddot{\theta}\end{Bmatrix} + \begin{bmatrix} k_{TLP} & 0 \\ 0 & m_k g\frac{l}{2} + m_p g l \end{bmatrix}\begin{Bmatrix} x \\ \theta \end{Bmatrix} = 0 \tag{3}$$

The following solution is obtained by assuming linear and angular motions as written in Eq. (4) and Eq. (5).

$$x = A_1 \sin \omega t \text{ ----> } \qquad \ddot{x} = -A_1\,\omega^2 \sin \omega t \tag{4}$$

$$\theta = A_2\, sin\, \omega \text{ ----> } \ddot{\theta} = -A_2\,\omega^2 \sin \omega t \tag{5}$$

The solution obtained is the Equation of motion as written in Eq. (6) and Eq. (7).

$$\begin{bmatrix} m_d + m_k + m_p & m_k\frac{l}{2} + m_p l \\ -m_d\frac{h}{2} + m_k\frac{l}{2} + m_p l & m_k\frac{l^2}{3} + m_p l^2 \end{bmatrix}\begin{Bmatrix}-A_1\omega^2\\ -A_2\omega^2\end{Bmatrix}\sin \omega t + \begin{bmatrix} k_{TLP} & 0 \\ 0 & m_k g\frac{l}{2} + m_p g l \end{bmatrix}\begin{Bmatrix} A_1 \\ A_2 \end{Bmatrix} sin\, \omega t = 0 \tag{6}$$

$$\begin{bmatrix} -m_d\omega^2 - m_k\omega^2 - m_p\omega^2 + k_{TLP} & -m_k\frac{l}{2}\omega^2 - m_p l\omega^2 \\ m_d\frac{h}{2}\omega^2 - m_k\frac{l}{2}\omega^2 - m_p l\omega^2 & -m_k\frac{l^2}{3}\omega^2 - m_p l^2\omega^2 + m_k g\frac{l}{2} + m_p g l \end{bmatrix} = 0 \tag{7}$$

2.3. Numerical solution

Eq. (7) which is known as the characteristic Equation, can be expressed in the matrix form in Eq. (8) using the state space form method [18]. The state-space form method can convert the second-order ordinary differential Equation to a first-degree ordinary differential Equation.

$$\begin{bmatrix} m_d{+}m_k{+}m_p & m_k\frac{l}{2}{+}m_p l \\ -m_d\frac{h}{2}{+}m_k\frac{l}{2}{+}m_p l & m_k\frac{l^2}{3}{+}m_p l^2 \end{bmatrix}\begin{Bmatrix}\ddot{x}\\ \ddot{\theta}\end{Bmatrix} + \begin{bmatrix} k_{top} & 0 \\ 0 & m_k g\frac{l}{2}{+}m_p g l \end{bmatrix}\begin{Bmatrix} x \\ \theta \end{Bmatrix} = \begin{Bmatrix} 0 \\ F_d \cos \omega t \end{Bmatrix} \tag{8}$$

Eq. (8) can be expressed in the form of Eq. (9), where [M] is the mass matrix, [K] is the stiffness matrix and $\bar{F}(t)$ is the force vector. Here $\dot{\vec{Y}}$ and $\vec{Y}$ are vectors represented by Eq. (10).

$$[M]\,\dot{\vec{Y}} + [K]\,\vec{Y} = \vec{F}_{(t)} \tag{9}$$

$$\dot{\vec{Y}} = \begin{Bmatrix} \ddot{x} \\ \dot{x} \end{Bmatrix}, \quad \vec{Y} = \begin{Bmatrix} \dot{x} \\ x \end{Bmatrix} \tag{10}$$

If Eq. (9) and Eq.(10) are solved simultaneously, then the solution is obtained using Eq. (11). Implementing numerical integration using the finite difference method, the solution is obtained as Eq. (12). The final solution is the sinusoidal wave Equation as given in Eq. (13).

$$\dot{\vec{Y}} = [M]^{-1}\left(\vec{F}_{(t)} - [K]\,\vec{Y}\right) \tag{11}$$

$$\frac{\vec{Y}_{(t+1)} - \vec{Y}_{(t)}}{t} = [M]^{-1}\left(\vec{F}_{(t)} - [K]\,\vec{Y}_{(t)}\right) \tag{12}$$

$$\vec{Y}_{(t+1)} = \vec{Y}_{(t)} + \quad t\left([M]^{-1}\left(\vec{F}_{(t)} - [K]\,\vec{Y}_{(t)}\right)\right) \tag{13}$$

2.4. Experimental studies

The experimental equipment is a pool of water as a medium for waves. The wave generator engine consists of an exciter driven by a connecting rod connected to an eccentric rotor. The waves oscillate at a frequency of 1.55 Hz. In this test, the horizontal motion (x-direction) of the existing TLP and TLP 2-DOF models were measured, respectively, and a comparative study was carried out. Displacement is measured using an ultrasonic sensor device. Figure 4. (a) shows water waves as a

medium, and Figure 4. (b) shows the new model (TLP 2-DOF) and the existing model. Test equipment specifications and wave specifications are shown in Table 2.

(a) (b)

Figure 4. (a) The test pool, (b) The new model (TLP 2-DOF), and the existing model.

Table 2. Wave conditions

Description	unit	value
Wave amplitude (A)	mm	50
Wavelength (λ)	mm	350
Wave frequency (f_w)	rad/s (Hz)	9,77 (1,55)

3. Results and Discussion

The dynamic response is expressed in the frequency domain. The discussion starts by determining the natural frequency and its relation to the resonance phenomenon. The advantages of TLP 2-DOF are shown in the graph for comparison with the existing model. In addition, it also discusses the effect of mass ratio (MD/m_p) on dynamic response, i.e., RAO on the primary mass (deck). The accuracy of the numerical method used was validated by comparing it with experimental data. Finally, the mass ratio (m_d/m_p) was optimized to minimize RAO.

3.1. Natural frequency

The natural frequency of the TLP 2-DOF model was obtained by solving the characteristic Eq., and the two lowest natural frequencies, f_1 and f_2 can be seen in Table 3. Compared to TLP on a real scale, this natural frequency is classified as significant. This is due to the small mass of the model. This is not a problem because the TLP scale has a large mass so that the natural frequency is minor. Natural Frequency is affected by the ratio of the mass of the deck to the mass of the pontoon (m_d/m_p). If the mass of the deck becomes smaller, then the natural frequency will be more significant. According to the well-known formula of natural Frequency, this is true, which is inversely proportional to the root square of the mass, as shown in Eq. (14). Here f_n is the natural frequency, k is the spring stiffness, and m is the mass.

$$f_n = \frac{1}{2\pi}\sqrt{\frac{k}{m}}. \quad (1)$$
(14)

Table 3. Frequency of the TLP 2-DOF model

Ratio (m_d/m_p)	Natural Frequency	
	f_1	f_2
1:3	0,587 hz	2,831 hz
1:2	0,562 hz	2,431 hz
2:3	0,539 hz	2,202 hz
1:1	0,501 hz	1,946 hz

3.2. Comparison of the new model vs. the existing model

Figure 5. shows a graph of the amplitude response of the new model and the existing model. Resonance occurs at the first natural frequency and the second natural frequency, around 0.587 Hz and 2.831 Hz. The graph was plotted for mass ratio (m_d/m_p) of 1:3. At resonance conditions, the dynamic response of the new model is only 0.4 times the existing model. It should be noted that the real TLP does not operate in the resonant frequency. Outside the resonance region, it can be seen that the RAO response is much smaller. This discussion concludes that this model (TLP-2-DOF) can be considered for application in extreme ocean waves.

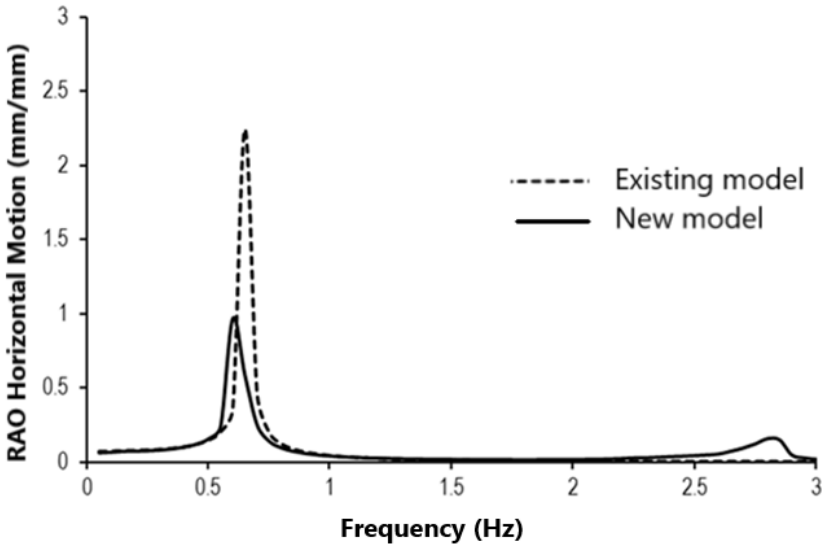

Figure 5. The dynamic response comparison between the new model and the existing model

3.3. Experimental validation

Experimental validation is required to check the accuracy of the numerical method. Figure 6. shows the dynamic response comparison between numerical and experimental. Although not the same, each graph has the same tendency and equally has a natural frequency of about 0.587 Hz. The slight deviations that occur are understandable because the experimental data allows various errors, such as human errors and equipment deviations. Thus it can be concluded that the numerical method used is accurate and correct.

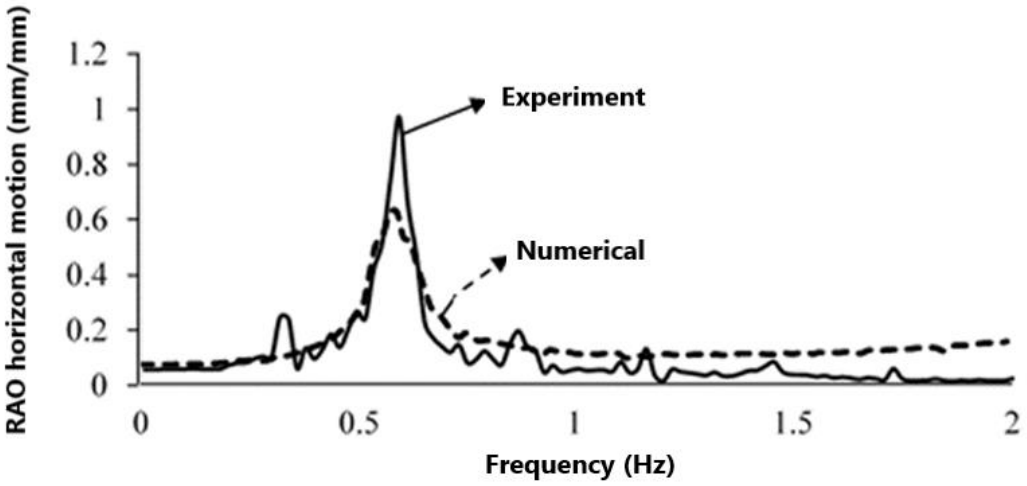

Figure 6. The dynamic response comparison between theoretical and experimental

3.4. Effect of mass ratio

The mass ratio in this discussion is the ratio of the mass of the deck to the mass of the pontoon (m_d/m_p). RAO graphs for various mass ratio values can be seen in Figure 7. The mass ratio significantly affects natural frequencies, around 0.587 Hz and 2.831 Hz, but not at other frequencies. This ratio affects RAO and becomes a maximum at m_d/m_p of about 0.67. In addition, the mass ratio affects the natural frequency, which is seen at resonance conditions; RAO peaks occur at different frequencies.

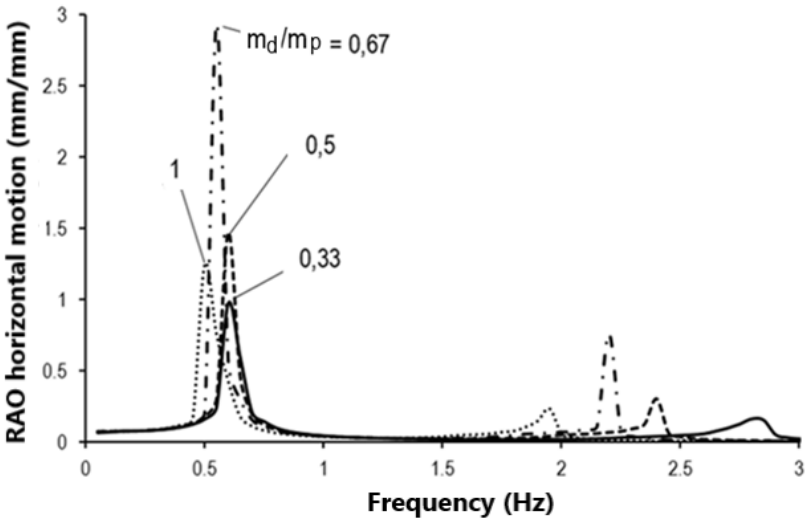

Figure 7. RAO graph for the various mass ratio (m_d/m_p) values

3.5. Optimization

To get the optimal design, optimization of the mass ratio (m_d/m_p) was carried out to minimize the RAO value on the deck. The optimization process is carried out using a numerical method. Figure 8. (a) shows recorded real-time displacement data, and Figure 8. (b) shows amplitude response in domain frequency. Amplitude response (RAO) to the mass ratio variation (m_d/m_p) is shown in Figure 9. In this case, the best ratio of the mass of the deck to the mass of the pontoon (m_d/m_p) is about 0.2.

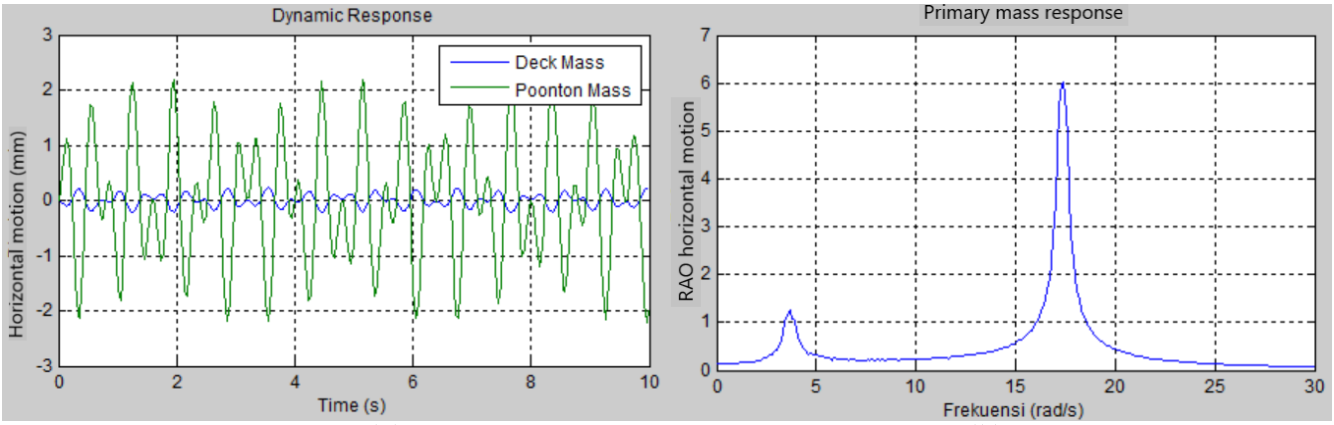

(a) (b)

Figure 8 (a). The recorded real-time displacement data, (b) The amplitude response in domain frequency

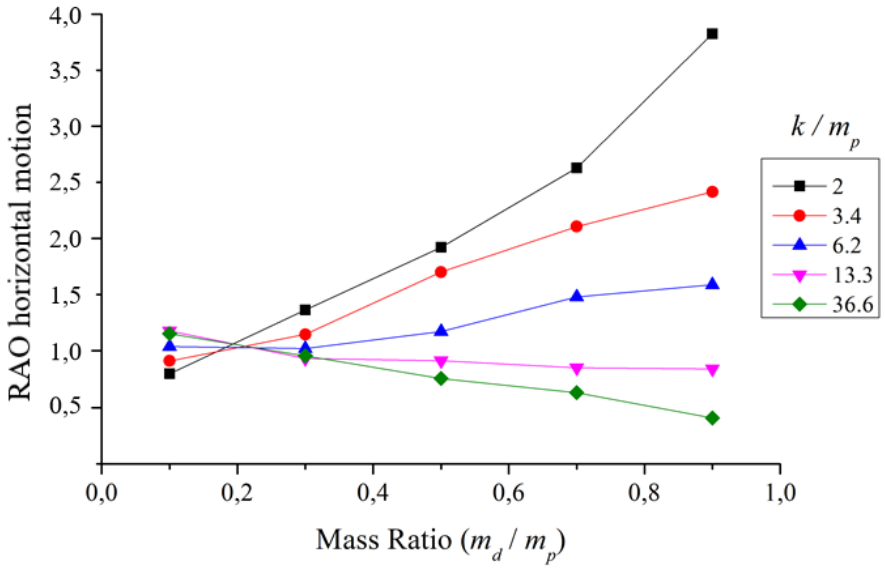

Figure 9. Amplitude response (RAO) to the mass ratio variation (m_d/m_p)

4. Conclusion

This paper proposes and discusses a new TLP model, called TLP 2-DOF, which has a more stable dynamic response when compared to the existing model. This can be seen in the respective RAO comparison graph, which depicts the RAO on the new model is relatively lower. At resonance conditions, this model can reduce RAO to about 67%. Parameters that affect TLP stability include the ratio of the mass of the deck to the mass of the pontoon (m_d/m_p). From the optimization process carried out using the numerical method, the optimum ratio is obtained at $m_d/m_p = 0.2$. Thus this model can be an alternative solution for field conditions with extreme waves.

Acknowledgment

The authors would like to acknowledge the Research Institute ("LPPM Universitas Lampung") for funding this research under the scheme of "Penelitian Unggulan BLU 2019".

References

[1] I. Senjanović , M. Tomić , and S. Rudan, "Investigation of nonlinear restoring stiffness in dynamic analysis of tension leg platforms," *Engineering Structure*, vol. 56, pp. 117– 125, 2013. doi: /10.1016/j.engstruct.2013.04.020

[2] X. Song, S. Wang, H. Li, and T. Li, "Investigation of the Hydrodynamic Performance of a Novel Semi-Submersible Platform with Multiple Small Columns," *Journal Ocean University China*, vol. 18, no. 1, pp. 108– 122, 2019. doi: org/10.1007/s11802-019-3679-y

[3] M. Rudman and P. W. Cleary, "Rogue wave impact on a tension leg platform: The effect of wave incidence angle and mooring line tension," *Ocean Engineering*, vol. 61, pp. 123– 138, Mar. 2013, doi: 10.1016/j.oceaneng.2013.01.006.

[4] M. Lou, C. Yu, and P. Chen, "Dynamic response of a riser under excitation of internal waves," *Journal Ocean University China*, vol. 14, no. 6, pp. 982– 988, Dec. 2015, doi: 10.1007/s11802-015-2701-2.

[5] M. R. Tabeshpour, A. Ahmadi, and E. Malayjerdi, "Investigation of TLP behavior under tendon damage," *Ocean Engineering*, vol. 156, pp. 580– 595, May 2018, doi: 10.1016/j.oceaneng.2018.03.019.

[6] J. Yu, S. Hao, Y. Yu, B. Chen, S. Cheng, and J. Wu, "Mooring analysis for a whole TLP with TTRs under tendon one-time failure and progressive failure," *Ocean Engineering*, vol. 182, pp. 360– 385, Jun. 2019, doi: 10.1016/j.oceaneng.2019.04.049.

[7] N. Abdussamie, Y. Drobyshevski, R. Ojeda, G. Thomas, and W. Amin, "Experimental investigation of wave-in-deck impact events on a TLP model," *Ocean Engineering*, vol. 142, pp. 541– 562, 2017. doi: 10.1016/j.oceaneng.2017.07.037

[8] S. Chandrasekaran and K. Yuvraj, "Dynamic analysis of a tension leg platform under extreme waves," *Journal Naval Architecture Marine Engineering*, vol. 10, no. 1, pp. 59– 68, Jun. 2013, doi: 10.3329/jname.v10i1.14518.

[9] S. Chandrasekaran and A. K. Jain, "Triangular configuration tension leg platform behavior under random sea wave loads," *Ocean Engineering*, vol. 29, no. 15, pp. 1895– 1928, 2002. doi: 10.1016/S0029-8018(01)00111-1

[10] S. Chandrasekaran, D. Kumar, and R. Ramanathan, "Dynamic response of tension leg platform with tuned mass dampers," *Journal Naval Architecture Marine Engineering*, vol. 10, no. 2, pp. 149– 156, 2013. doi: 10.3329/jname.v10i2.16184

[11] D. Qiao, B. Li, and J. Ou, "Use of different mooring models on global response analysis of an innovative deep draft platform," *Journal Ocean University China*, vol. 13, no. 2, pp. 215– 222, 2014. doi: 10.1007/s11802-014-2012-z

[12] H. H. Lee and P.-W. Wang, "Analytical solution on the surge motion of tension-leg twin platform structural systems," *Ocean Engineering*, vol. 27, no. 4, pp. 393– 415, 2000. doi: 10.1016/S0029-8018(98)00047-X

[13] Y.-M. Choi, B. W. Nam, S. Y. Hong, D. W. Jung, and H. J. Kim, "Coupled motion analysis of a tension leg platform with a tender semi-submersible system," *Ocean Engineering*, vol. 156, pp. 224– 239, 2018. doi: 10.1016/j.oceaneng.2018.01.031

[14] P. Su, J. Wu, S. Liu, and J. Jiang, "Study on the dynamics of the two-degree-of-freedom system with variable stiffness magnetic isolator," *Journal Vibroengineering*, vol. 20, no. 1, pp. 116– 126, 2018, doi: 10.21595/jve.2017.18847.

[15] V. Piccirillo, A. M. Tusset, and J. M. Balthazar, "Optimization Of Dynamic Vibration Absorbers Based On Equal-Peak Theory," *Latin American Journal Solids and Structure*, vol. 16, no. 4, p. e184, 2019, doi: 10.1590/1679-78255285.

[16] Y. Shen, X. Wang, S. Yang, and H. Xing, "Parameters Optimization for a Kind of Dynamic Vibration Absorber with Negative Stiffness," *Mathematical Problems in Engineering*, vol. 2016, pp. 1– 10, 2016, doi: 10.1155/2016/9624325.

[17] B. Utomo and M. Iqbal, " Vertical Motion Optimization of Series 60 Hull Forms Using Response Surface Methods," *Kapal: Jurnal Ilmu Pengetahuan dan Teknologi Kelautan*, vol. 17, no. 3, pp. 130– 137, Oct. 2020, doi: 10.14710/kapal.v17i3.33212.

[18] H. G. Harno, "On the Synthesis of a Linear Quadratic Controller for a Quadcopter," *International Journal of Applied Sciences and Smart Technologies*, vol. 01, no. 02, pp. 101– 112, 2019, doi: 10.24071/ijasst.v1i2.1919.